Earth and Planetary Science Letters, 105 (1991) 110–126
Elsevier Science Publishers B.V., Amsterdam

[CH]

Sr and Nd isotopic evidence for punctuated clay diagenesis, Texas Gulf Coast

Matthias Ohr, Alex N. Halliday and Donald R. Peacor

Department of Geological Sciences, University of Michigan, Ann Arbor, MI 48109, USA

Received October 10, 1990; revised and accepted April 16, 1991

ABSTRACT

We report Rb-Sr, Sm-Nd and mineralogical data for leached whole rock, < 2 μm and < 0.1 μm clay size fractions of lower- to mid-Tertiary shales spanning the smectite/illite transition, from a single deep well in the Texas Gulf Coast. The abrupt transition at 2400 m, from smectite- to illite-dominated assemblages is accompanied by a marked increase in $^{87}Sr/^{86}Sr$ from 0.708 to 0.711 in exchangeable sites. Leached authigenic illite from the < 0.1 μm fraction, sampled from below the smectite/illite transition, defines a Rb-Sr isochron age of 34.8 ± 2.0 Ma. These data are consistent with a single episode of authigenic illite precipitation over a depth range of > 1200 m, independent of the duration of burial. The exchangeable Sr in the clay has remained an open system and has undergone isotopic exchange since that time. Minimum fluid/rock ratios of 0.2 to 2 are modeled from Sr isotopic data, consistent with rock-dominated, open system diagenesis. Leachates and residues of the < 0.1 μm fraction, below the smectite/illite transition appear to have achieved Nd isotopic equilibrium during clay diagenesis, and show no signs of subsequent exchange. The clay residues have low $^{147}Sm/^{144}Nd$ (< 0.085), indicating that authigenic illite has a lower Sm/Nd ratio than its bulk rock protolith. Conversely the coexisting exchangeable REE inventory has elevated Sm/Nd, as reflected by leachate $^{147}Sm/^{144}Nd$ as high as 0.188. This Sm/Nd fractionation, in conjunction with the preserved isotopic equilibrium may be useful for dating diagenesis and associated fluid–rock interaction in older rocks.

1. Introduction

Diagenesis and low grade metamorphism of argillaceous sediments are commonly thought to be gradual processes related to depth and longevity of burial. The Gulf Coast sedimentary succession has long been considered to be a type sequence in this context, as described by Hower et al. [1]. Recently, this view of clay diagenesis has been challenged by Morton [2] who pointed out the discontinuous character of diagenesis. In fact, Oliver [3] argued that a wide range of low-temperature processes inclusive of clay diagenesis may be episodic in nature and the result of tectonically controlled fluid flow. In order to understand complex diagenetic systems in both time and space, it is critical to find ways of dating fluids and the products of their interaction with the crust. Dissolution of smectite-rich precursor clay and precipitation of authigenic illite are instrumental in diagenesis [4] and may allow the establishment of isotopic equilibrium with the coexisting pore fluid. In this study the viability of Rb-Sr and Sm-Nd dating of clay diagenesis is explored, as the evaluation of models of diagenesis depends on the ability to constrain the timing and mass transfer history of the mineral transformations involved.

2. The smectite/illite transition

Numerous workers have evaluated the depth-related mineralogical changes that occur during diagenesis of Gulf Coast argillaceous sediments (e.g. [1,5–8]). The most prominent change in clay mineral assemblages has been summarized as [1]:

$$\text{smectite} + Al^{3+} + K^{+} = \text{illite} + Si^{4+} + H_2O$$

More complete versions of this reaction have also been suggested [9]. Mixed-layer illite/smectite (hereafter simply called authigenic illite) forming as a reaction product of smectite has up to 50% of interlayer cation sites vacant, develops as the $1M_d$ polytype and occurs as small crystallites having a high density of dislocations [10]. Illite is

0012-821X/91/$03.50

metastable [11] and, with increasing grade, changes in composition toward that of muscovite, in a process likened by some to an Ostwald step rule process [4] or Ostwald ripening [12,13].

The nature of the smectite to illite transition has been documented in many areas (e.g. [1,8,14–17]). An observation common to all studies is the lack of a progressive increase of%illite in illite/smectite mixed-layer clay (I/S clay) as a function of burial depth. Instead, smectite-rich I/S clay is replaced by illitic I/S clay (I < 90%) over a narrow depth interval. The transition has traditionally been viewed as an equilibrium-controlled process of continuous clay growth that is governed by local parameters such as thermal gradient and availability of potassium [1,18]. In contrast, Morton [2,19] suggested that punctuated interaction of smectite with pore fluids results in episodic precipitation of authigenic illite over a large depth or regional range. The discontinuous mineralogical gradient was interpreted as a kinetic effect with the reaction rate being greatest at high temperatures.

3. Dating clay diagenesis

The proposed models of clay diagenesis are fundamentally distinct as they imply different time scales over which diagenetic reactions proceed, namely protracted clay growth with progressive burial versus episodic growth over a large depth range. Both the Rb-Sr and K-Ar isotopic dating techniques are frequently employed to evaluate the appropriateness of these models (e.g. [2,19–26]). Most radiogenic isotope studies of low-grade pelites have revealed younger Rb-Sr and K-Ar ages in finer grain size fractions. The problem of discordant ages related to Ar and Sr inherited from detrital contamination in coarse size fractions was recognized early on [27,28]. However, even for pure authigenic separates, the presence and variable proportions of multiple generations of authigenic clay and micas can present additional uncertainties and this is a particular problem for evaluating protracted clay growth or progressive recrystallization of phyllosilicates in a prograde environment. Alternatively, the generally younger ages of fine-grained clay and mica may relate to incomplete retentivity of the daughter elements. K-Ar ages of illite, for example, may not necessarily define the time of illitization, but rather that of the last thermal event affecting the system. There seems to be agreement, however, that fine-grained clays, at temperatures below 100°C, are probably retentive with respect to Ar [29,30], and certainly with regard to Sr.

The Rb-Sr method of dating clays has been outlined by Clauer [31,32]. Morton [2,19] presented Rb-Sr isochrons from Tertiary Gulf Coast sediments and Devonian shales, respectively, with ages significantly younger than the time of deposition. Erwin and Long [25] used Rb-Sr mixing lines to suggest that diagenesis immediately followed deposition in Permian shales and sandstones from Texas. A similar approach used by Liewig et al. [23] and Clauer et al. [26] resulted in ages greater than the depositional age of the clays. These widely varying results reflect either compositional heterogeneities in the separates, uncertainties in assessing the degree of Sr isotopic equilibrium between various structural sites in mixed-layer clays, or a non-uniform Sr reservoir in the coexisting fluids. Both non-systematic and systematic factors contribute to uncertainties in interpretation. Hence the reliability of an age is enhanced by (a) mineralogical and chemical characterization of the clay separates to minimize problems of contamination and heterogeneity, and (b) fully addressing the possibility of isotopic disequilibrium within the clay separates.

4. Study location and sample description

The samples used in this study were separated from shales recovered from the Socony Mobil Oil Company No.1 Zula E. Boyd well, DeWitt County, Texas Gulf Coast (Fig. 1). This well penetrates a lower Miocene to Paleocene sequence of shales and sandstones to a depth of 3650 m (12,000 ft), the main geologic unit being the Eocene Wilcox Group. At this locality, the Miocene–Oligocene boundary is at about 430 m (1400 ft) depth, the Oligocene–Eocene boundary is found at 1220 m (4000 ft), and the upper boundary of the Paleocene is approximately at 3050 m (10,000 ft) depth. Samples used for this study were taken from the original material studied and described in detail by Freed and Peacor [8,33], allowing direct comparison. The main compositional trend in the clay

mineral assemblage from the Zula Boyd well is summarized in Fig. 1a: the smectite/illite transition occurs in a narrow interval between 2130 m and 2440 m, from smectite-rich I/S clay (< 50% illite) to an assemblage dominated by authigenic I/S with 80–90% illite.

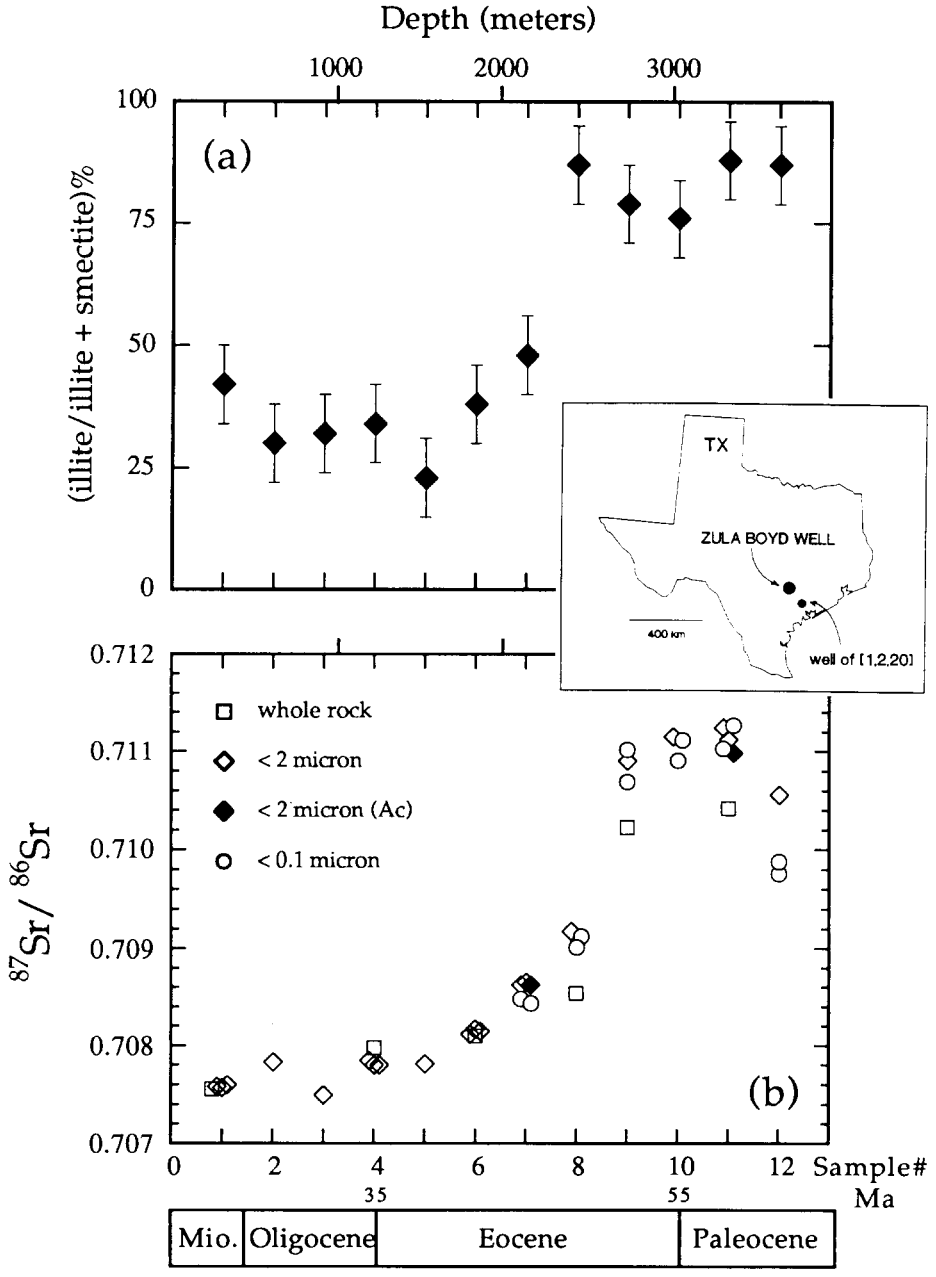

Fig. 1. (a) Percentage of non-expandable layers in mixed-layer I/S clay is plotted against depth, Zula Boyd well, Texas (see insert). Size fraction is < 2 μm. The transition from < 50% non-expandable I/S to > 80% non-expandable I/S occurs discontinuously between 2130 m and 2440 m [8]. (b) $^{87}Sr/^{86}Sr$ of exchangeable Sr (leached Sr) from all size fractions is also a discontinuous function of depth, corresponding to the depth of the smectite/illite transition. Sample numbers refer to well depth in thousands of feet, and approximate time markers are given.

5. Techniques

The separation of authigenic illite takes advantage of the difference in grain size between detrital clay and finer authigenic clay. Drill cuttings were soaked in distilled water, gently disaggregated using mortar and pestle, and placed in an ultrasonic waterbath. The resulting suspension was decanted and, if flocculation was observed, redispersed with dilute sodium-metahexaphosphate solution (the Sr and Rb blanks being less than 20% of the total procedure blank). Initial separation of the < 2 μm fraction was achieved by repeated gravity settling, and separation of the < 0.1 μm fraction was performed on a high-speed Sorvall RC2-B centrifuge. The predicted grain size and purity of selected separates were confirmed by scanning transmission electron microscopy.

A fundamental problem in dating fine-grained sedimentary samples is the presence of non-radiogenic Sr in exchangeable clay sites, adsorbed onto clay surfaces, and in soluble authigenic phases. In order to remove that Sr component, clay separates were leached using cold, distilled 1*N* HCl, and, for comparison, using 10% acetic acid for selected samples. The duration of leaching varied between 30 minutes (< 2 μm fraction) and 20 hours (whole rock and < 0.1 μm fraction).

All isotopic composition and isotope dilution measurements were performed in the Radiogenic Isotope Geochemistry Laboratory at the University of Michigan. Typical sample size prior to leaching was 10–40 mg. Leachate and residue were separated by centrifuging, and the residue rinsed repeatedly with deionized water, dried and reweighed. Residues were digested in a mixture of concentrated distilled HF, $HClO_4$, and HNO_3. Total procedure blanks were < 200 pg for Sr, and < 50 pg for Nd. $^{87}Rb/^{86}Sr$ and $^{147}Sm/^{144}Nd$ were determined by isotope dilution, using mixed ^{87}Rb-^{84}Sr, and ^{149}Sm-^{150}Nd spikes. $^{87}Rb/^{86}Sr$ ratios are accurate to better than 1%, and $^{147}Sm/^{144}Nd$ ratios to about 0.1%. Most $^{87}Sr/^{86}Sr$ ratios and all $^{143}Nd/^{144}Nd$ ratios were determined on totally spiked aliquots, and are presented with a correction for spike contributions. Details of ion exchange and mass spectrometric procedures can be found in Halliday et al. [34]. All mass spectrometric measurements were performed on two V.G. Sector multicollector thermal ionization mass spectrometers, yielding compatible standard values of 0.710248 ± 10 for $^{87}Sr/^{86}Sr$ of NBS 987 ($n = 77$), and 0.511868 ± 10 ($\epsilon_{Nd} = -15.0 \pm 0.2$) for $^{143}Nd/^{144}Nd$ of La Jolla ($n = 27$). These uncertainties for the standards are expressed as 2σ standard deviations.

Grain sizes in the < 0.1 μm separates (calculated as the average of the long and short aspect of the crystal), chemical compositions and morphologies of individual grains were determined at the Electron Microbeam Analysis Laboratory of the University of Michigan, using a Philips CM 12 STEM fitted with a Kevex Quantum EDS system. Selected samples were ultrasonically disaggregated and the suspended particles spread over a thin "holey carbon" membrane which rests on a fine Cu mesh. Normal laboratory procedures allow the determination of chemical compositions with accuracies approaching those of microprobe analyses for most elements [12].

6. Results

6.1. Mineralogical relations

The occurrence of small, thin hexagonal illite-rich crystals has been documented in whole rock samples throughout the section of the Zula Boyd well [8]. In this study the majority of the < 0.1 μm fraction is also comprised of such euhedral to subhedral hexagonal grains, with only minor populations of irregularly shaped clay grains. Chlorite is very rare, but minute grains of apatite, rutile, and titanite are common in the < 0.1 μm fraction. In some cases, illite has grown around small, titaniferous grains. Representative images of these hexagonal grains, and a spectrum of measured grain sizes are presented in Fig. 2. Grain shapes are distinctly polyhedral (Fig. 2a), ranging from well defined hexagonal outlines to less regular shapes; detrital smectite with its characteristically ill-defined and diffuse texture is absent. Comparison of grain shapes before and after leaching indicates that leaching can produce slightly less well-defined grains, i.e,. the grain edges tend to be wavy and the corners are more rounded (Fig. 2b). Abundant subhedral grains result from grain fragmentation (probably occurring during sample preparation), and some of the more irregular grain shapes derive from superposition of

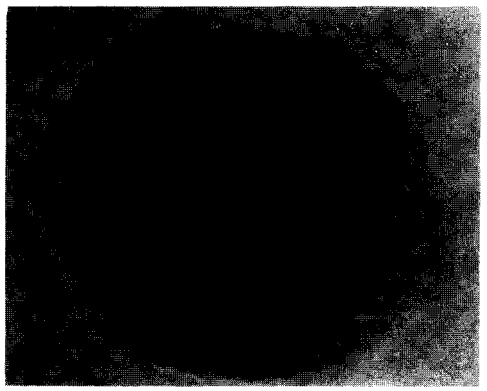

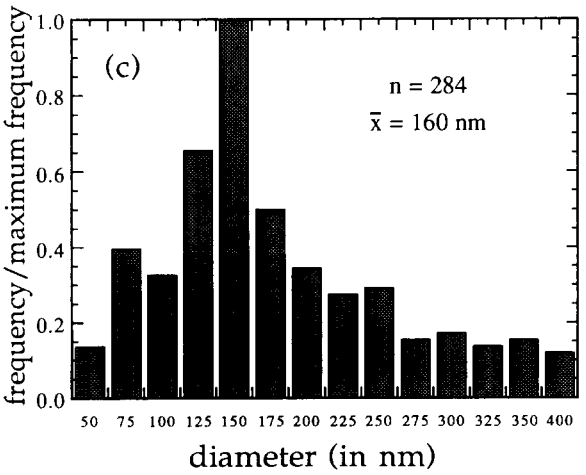

Fig. 2. (a) STEM photograph of hexagonal illite crystal from sample 11U (3350 m, untreated). (b) STEM photograph of acid-leached illite crystal from sample 11R (3350 m, residue). The scale bar is 0.1 μm for both (a) and (b). (c) Histogram of grain diameters in 11U, measured as (a+b)/2. The mean diameter is 0.16 μm. The size fraction is < 0.1 μm (e.s.d.) for (a), (b), and (c).

crystallites in random orientation. Grain diameters in each specimen are similar to sizes predicted by the modified Stoke's equation for centrifugal gravity settling [35]. The mean grain size is about 0.16 μm (separated at 0.1 μm e.s.d), with a somewhat skewed distribution toward larger grains, the upper limit being around 0.4 μm (Fig. 2c). However, as very small grains formed clumps during the preparation of the STEM specimens, the abundance of measured grains smaller than about 0.05 μm is likely to be under-represented.

Structural formulae of illite grains of selected samples, normalized to 6 cations in the tetrahedral and octahedral sites, and assuming a dioctahedral structure are shown in Table 1. The dominant interlayer cation present is K, with Ca and Na mostly absent. The total deficiency in negative charge is calculated as the sum of the tetrahedral sites occupied by Al, and the octahedral sites occupied by Mg. The mean of the calculated positive interlayer charge of untreated samples 8 and 11 is +0.75. and +0.80, respectively, whereas the mean for the corresponding residues is +0.74 and +0.65 (Table 1).

6.2. *Rb-Sr isotopic data*

All Sr isotopic data are presented in Table 2. Three sample sets were analyzed: whole rock, < 2 μm, and < 0.1 μm size fractions. Sample numbers denote depth within the well in thousands of feet (i.e, samples 1 through 12 range from 1000 ft to 12,000 ft depth). Modifiers denote leachates (L), residual samples after leaching (R), and untreated samples (U).

A plot of $^{87}Sr/^{86}Sr$ of all leachates as a function of stratigraphic depth is given in Fig. 1b. We find a close correlation between the isotopic composition of exchangeable Sr and clay assemblages, in that the depth of the abrupt increase in $^{87}Sr/^{86}Sr$ of the leachates approximately coincides with the depth of the smectite/illite transition (Fig. 1). $^{87}Sr/^{86}Sr$ of exchangeable Sr from pre-transition samples is approximately constant between 0.7075 and 0.7079; between 1830 m and 2440 m $^{87}Sr/^{86}Sr$ ratios increase rapidly, and reach another plateau at about 0.711 for the deepest samples ranging from 2740 m to 3660 m. Leachate isotopic compositions of individual samples, however, are largely insensitive to variations in grain size, length

TABLE 1

Analytical electron microscopy data

Sample 8	UNTREATED														mean	RESIDUE								mean
Size in nm[a]	75	85	90	95	100	120	130	160	195	200	210	225	270	300	164	85	100	115	120	175	180	245	280	163
IV[b]: Si	3.74	3.26	3.57	3.57	3.46	3.50	3.46	3.56	3.64	3.39	3.48	3.39	3.39	3.30	3.48	3.41	3.49	3.52	3.28	3.62	3.52	3.58	3.13	3.44
Al	0.26	0.74	0.43	0.43	0.54	0.50	0.54	0.44	0.36	0.61	0.52	0.61	0.61	0.70	0.52	0.59	0.51	0.48	0.72	0.38	0.48	0.42	0.87	0.56
VI[c]: Al	1.31	1.80	1.54	1.42	1.53	1.37	1.76	1.79	1.43	1.62	1.63	1.48	1.54	1.81	1.57	1.64	1.66	1.60	1.73	1.47	1.35	1.56	1.81	1.60
Mg	0.31	0.12	0.25	0.27	0.22	0.28	0.15	0.11	0.26	0.28	0.20	0.31	0.24	0.09	0.22	0.15	0.21	0.25	0.15	0.21	0.20	0.26	0.09	0.19
Fe^{3+}	0.38	0.07	0.20	0.30	0.25	0.35	0.11	0.11	0.31	0.09	0.17	0.21	0.23	0.09	0.21	0.22	0.14	0.14	0.12	0.32	0.45	0.18	0.10	0.21
charge deficiency[d]	0.57	0.86	0.68	0.70	0.76	0.78	0.69	0.55	0.62	0.89	0.72	0.92	0.85	0.79	0.75	0.74	0.72	0.73	0.87	0.59	0.68	0.68	0.96	0.74
$K_{measured}$	0.13	0.05	0.13	0.17	0.11	0.16	0.13	0.09	0.31	0.40	0.08	0.28	0.24	0.06	0.17	0.12	0.08	0.18	0.13	0.20	0.21	0.49	0.59	0.25
$K_{m/p.i.c}$[e]	0.23	0.06	0.19	0.24	0.14	0.21	0.19	0.16	0.50	0.45	0.11	0.30	0.28	0.08	0.23	0.16	0.11	0.25	0.15	0.34	0.31	0.72	0.61	0.34

Sample 11	UNTREATED								mean	RESIDUE																	mean
Size in nm[a]	80	100	110	135	140	210	240	250	158	60	65	70	75	80	90	105	110	115	120	135	160	185	190	200	210	240	130
IV[b]: Si	3.60	3.45	3.30	3.52	3.52	3.47	3.45	3.46	3.46	3.46	3.56	3.50	3.61	3.62	3.50	3.56	3.55	3.41	3.63	3.50	3.51	3.50	3.55	3.62	3.56	3.35	3.53
Al	0.40	0.55	0.70	0.48	0.48	0.53	0.55	0.54	0.54	0.54	0.44	0.50	0.39	0.38	0.50	0.44	0.45	0.59	0.37	0.50	0.49	0.50	0.45	0.38	0.44	0.65	0.47
VI[c]: Al	1.47	1.47	1.53	1.62	1.45	1.47	1.57	1.55	1.51	1.60	1.76	1.78	1.75	1.76	1.83	1.72	1.83	1.76	1.72	1.61	1.79	1.70	1.77	1.66	1.67	1.68	1.72
Mg	0.38	0.25	0.25	0.23	0.30	0.27	0.25	0.22	0.27	0.28	0.11	0.21	0.16	0.13	0.10	0.17	0.13	0.14	0.16	0.26	0.11	0.17	0.15	0.19	0.20	0.19	0.17
Fe^{3+}	0.25	0.28	0.21	0.14	0.25	0.26	0.18	0.22	0.22	0.12	0.13	0.11	0.13	0.12	0.07	0.11	0.13	0.10	0.12	0.13	0.09	0.13	0.08	0.15	0.13	0.13	0.11
charge deficiency[d]	0.78	0.80	0.95	0.71	0.78	0.80	0.80	0.76	0.80	0.82	0.55	0.71	0.55	0.51	0.60	0.61	0.58	0.73	0.53	0.76	0.60	0.67	0.60	0.57	0.64	0.84	0.65
$K_{measured}$	0.65	0.63	0.68	0.58	0.65	0.54	0.56	0.57	0.61	0.61	0.24	0.18	0.24	0.18	0.09	0.16	0.16	0.11	0.28	0.20	0.09	0.27	0.19	0.17	0.26	0.16	0.21
$K_{m/p.i.c}$[e]	0.83	0.79	0.72	0.82	0.83	0.68	0.70	0.75	0.77	0.74	0.44	0.25	0.44	0.35	0.15	0.26	0.28	0.15	0.53	0.26	0.14	0.40	0.32	0.30	0.41	0.19	0.32

a: diameter is calculated as the average of short and long aspect of the grain, (a + b)/2.
b,c: tertrahedral sites and octahedral sites, respectively.
d: negative charge deficiency is inferred to equal the positive interlayer charge = p.i.c.
e: Kmeasured / positive interlayer charge

TABLE 2

Rb-Sr isotopic data

whole rock		UNTREATED[a]				LEACHATE						RESIDUE				
Depth (m)	#[b]	$^{87}Rb/^{86}Sr$	$^{87}Sr/^{86}Sr$	Rb	Sr	$^{87}Rb/^{86}Sr$	$^{87}Sr/^{86}Sr$	Rb	Sr	%L[c]	%Sr_L[d]	$^{87}Rb/^{86}Sr$	$^{87}Sr/^{86}Sr$	Rb	Sr	Age_{L-U-R}[e]
305	1	0.45	0.7087			0.02073	0.70756 (2)	7.26	1008	35	86	3.371	0.71635 (4)	101	86.1	184.5
1220	4	1.50	0.7123			0.1486	0.70798 (4)	65.4	1268	29	86	3.610	0.71887 (1)	107	85.4	221.2
1829	6	1.15	0.7123			0.06904	0.70810 (4)	36.5	1521	9.2	66	3.384	0.72074 (1)	92.7	79.0	268.0
2438	8	1.42	0.7166			0.1032	0.70854 (4)	32.3	901	10	54	2.958	0.72607 (3)	87.3	85.1	431.1
2743	9	2.95	0.7174			0.2392	0.71023 (1)	48.5	584	5.4	26	3.805	0.71965 (2)	125	94.6	185.8
3353	11	2.27	0.7169			0.1840	0.71042 (1)	30.5	478	6.9	26	2.947	0.71892 (3)	103	101	216.3
<2 micron																
305	1	0.432	0.70822 (2)	71.6	477	0.01622	0.70757 (1)				73	3.309	0.71245 (3)			104.7 (1.7)
610	2	1.740	0.70881 (2)	139	230	-----	0.70783 (2)				---	4.702	0.71122 (3)			------
914	3	1.465	0.71016 (2)	87.2	172	-----	0.70749 (1)				---	4.304	0.71549 (3)			------
1219	4	1.416	0.71125 (4)	94.5	193	0.09026	0.70780 (1)				65	4.371	0.71781 (2)			169.9 (8.5)
1524	5	1.168	0.71103 (1)	109	269	-----	0.70781 (1)				---	1.346	0.71751 (2)			------
1829	6	1.008	0.71140 (2)	88.8	254	0.06438	0.70815 (1)				54	2.677	0.71759 (2)			249.3 (5.9)
2134	7	2.070	0.71403 (4)	81.4	113	0.1378	0.70863 (4)				47	3.835	0.71965 (2)			205.3 (7.4)
2438	8	1.181	0.71274 (3)	54.8	134	0.09006	0.70918 (1)				48	4.066	0.72102 (2)			216.5 (9.7)
2743	9	1.988	0.71463 (3)	95.0	137	0.1303	0.71091 (2)				39	4.806	0.71758 (1)			not aligned
3048	10	2.380	0.71482 (4)	102	123	0.2802	0.71116 (3)				26	4.336	0.71739 (2)			112.0 (9.9)
3353	11	2.745	0.71559 (3)	108	113	0.1527	0.71113 (1)				25	3.906	0.71794 (1)			125.0 (3.3)
3658	12	2.266	0.71471 (3)	130	165	0.08782	0.71056 (2)				34	3.558	0.71808 (2)			145.5 (9.9)
<0.1 micron																
2134	7	-----	----------	---	---	0.1047	0.70848 (2)	51.9	1426	7.5	72	5.931	0.71661 (3)	94.1	45.7	98.2
2438	8	2.034	0.71140 (5)	112	159	0.1979	0.70912 (2)	98.5	1405	8.5	72	6.352	0.71788 (1)	113	51.4	98.4 (5.0)
2743	9	3.744	0.71367 (2)	168	129	0.1833	0.71069 (1)	49.3	775	9.8	68	12.33	0.72074 (1)	171	39.9	58.5 (0.3)
3048	10	-----	----------	---	---	0.2626	0.71091 (1)	43.9	571	4.8	49	12.46	0.72092 (3)	129	29.7	57.8
3353	11	3.661	0.71399 (2)	151	118	0.1886	0.71103 (1)	139	2117	3.4	70	14.02	0.72176 (1)	154	31.6	56.4 (2.8)
3658	12	4.321	0.71429 (2)	163	103	1.349	0.70976 (1)	1215	2595	2.5	68	12.55	0.72090 (1)	139	31.8	not aligned

Leaching (<2 micron)		LEACHATE		RESIDUE	
		$^{87}Rb/^{86}Sr$	$^{87}Sr/^{86}Sr$	$^{87}Rb/^{86}Sr$	$^{87}Sr/^{86}Sr$
2134	7 (HCl)	0.1451	0.70866 (4)	3.895	0.71947 (1)
	7 (Ac)	0.1063	0.70863 (2)	3.028	0.71707 (5)
	T_{L-R} = 202.3 (2.2)				
3353	11 (HCl)	0.2518	0.71125 (2)	3.955	0.71817 (2)
	11 (Ac)	0.04379	0.71099 (2)	3.760	0.71766 (3)
	T_{L-R} = 128.4 (3.3)				

a: whole rock untreated sample is re-integrated from leachate and residue data.
b: sample numbers refer to well depth in thousands of feet.
c: wt.% leachate relative to untreated sample weight.
d: wt.% Sr leached relative to total Sr inventory.
e: apparent leachate-untreated-residue age in Ma [54]. 1σ error indicates fit of mass balance. Ages without errors correspond to leachate-residue tie lines.

of leaching and acid strength (Fig. 1b). The effects of leaching with acid of different strength (1*N* HCl and 10% acetic acid) were compared: higher $^{87}Rb/^{86}Sr$ and $^{87}Sr/^{86}Sr$ ratios of the HCl-leached residues, combined with relatively constant isotopic composition of the corresponding leachates (Table 2), indicate that more complete leaching does not preferentially contaminate the leachates with radiogenic ^{87}Sr, confirming previous studies (e.g. [36,37]).

Rb-Sr data for the < 2 μm and < 0.1 μm size fractions are presented in Fig. 3a and b. While the scatter among the < 2 μm residues is considerable, the < 0.1 μm residues from depths of 2440 m and greater show a more regular pattern. Below the smectite/illite transition (samples 8 through 12) we observe a linear relationship between

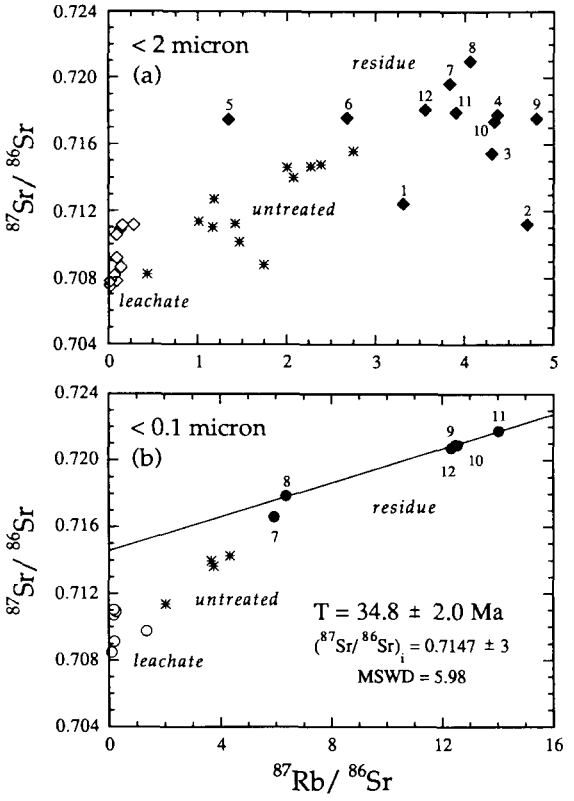

Fig. 3. (a) < 2 μm fraction. The scatter in residue data is due to variable amounts of detrital material and differential response to leaching. (b) < 0.1 μm fraction. Sample residues 8 through 12 (depths greater than smectite/illite transition) define an isochron age of 34.8 ± 2.0 Ma (regressed using [54]). Exchangeable Sr in the leachates is not in isotopic equilibrium with non-exchangeable Sr in the clay residues.

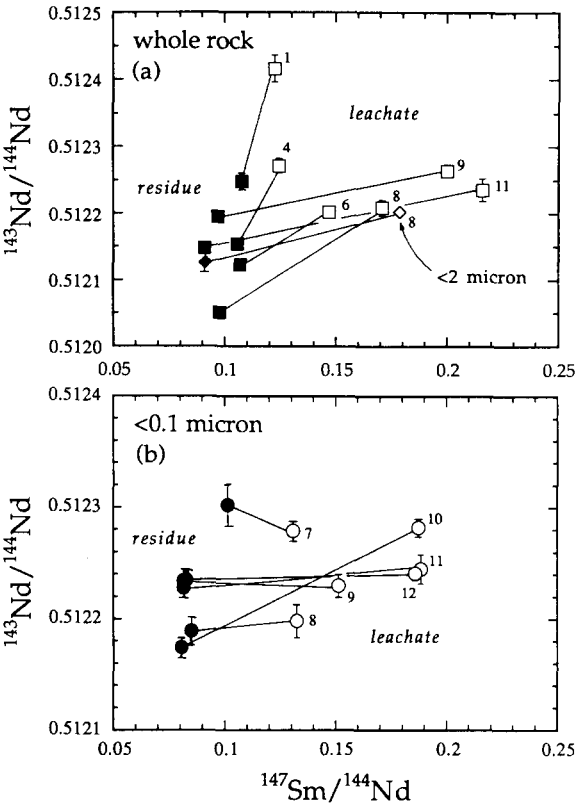

Fig. 4. (a) Whole rock samples. Younging of apparent residue–leachate ages (Table 3) with increasing depth indicates progressive isotopic equilibration as a result of dissolution of detritus and precipitation of authigenic clay. (b) < 0.1 μm fraction. Leachates and corresponding residues display Sm/Nd fractionation, but have identical $^{143}Nd/^{144}Nd$ (excluding sample 10), suggesting young Nd isotopic equilibration during diagenesis.

$^{87}Sr/^{86}Sr$ and $^{87}Rb/^{86}Sr$, the slope of which corresponds to an apparent Rb-Sr age of 34.8 ± 2.0 Ma (MSWD = 5.98). The initial $^{87}Sr/^{86}Sr$ ratio of 0.7147 ± 3 is significantly greater than the coexisting leachate compositions.

6.3. *Sm-Nd isotopic data*

Sm-Nd data for a selected range of bulk sediment samples, < 2 μm and < 0.1 μm fractions, are presented in Table 3. Leachate–residue pairs of whole rock samples are not in isotopic equilibrium, although with increasing depth, their respective $^{143}Nd/^{144}Nd$ converge and $^{147}Sm/^{144}Nd$ ratios diverge (Fig. 4a). In contrast, most leachate–residue pairs of the < 0.1 μm fraction

TABLE 3

Sm-Nd isotopic data

whole rock		UNTREATED[a]			LEACHATE							RESIDUE						
Depth (m)	#[b]	$^{147}Sm/^{144}Nd$	$^{143}Nd/^{144}Nd$	ε_{Nd}[c]	$^{147}Sm/^{144}Nd$	$^{143}Nd/^{144}Nd$	ε_{Nd}	Sm	Nd	%L[d]	Nd_L[e]	$^{147}Sm/^{144}Nd$	$^{143}Nd/^{144}Nd$	ε_{Nd}	Sm	Nd	T_{DM}[f]	Age_{L-R} (Ma)[g]
305	1	0.1164	0.51235	-5.6	0.12229	0.512417 (20)	-4.3	7.43	36.7	36	62	0.10774	0.512248 (12)	-7.6	2.26	12.7	1.14	1766 ± 244
1219	4	0.1140	0.51221	-8.3	0.12445	0.512272 (11)	-7.1	8.44	41.0	32	46	0.10541	0.512154 (5)	-9.4	3.85	22.1	1.24	945 ± 97
1829	6	0.1142	0.51214	-9.7	0.14686	0.512202 (9)	-8.5	13.3	54.6	13	22	0.10681	0.512123 (8)	-10.1	5.09	28.8	1.30	301 ± 46
2438	8	0.1155	0.51209	-10.7	0.17075	0.512209 (12)	-8.4	18.5	65.5	10	16	0.097706	0.512051 (8)	-11.5	3.95	40.3	1.30	330 ± 31
2743	9	0.1134	0.51220	-8.5	0.20002	0.512264 (8)	-7.3	26.5	80.1	6.7	16	0.096847	0.512195 (8)	-8.6	4.74	29.6	1.10	102 ± 17
3353	11	0.1155	0.51216	-9.3	0.21582	0.512236 (17)	-7.8	30.0	84.1	7.6	20	0.090681	0.512148 (9)	-9.5	4.22	28.1	1.11	107 ± 24
< 2 micron																		
2438	8	0.1058	0.51214	-9.6	0.17855	0.512203 (9)	-8.5	27.8	94.2	10	29	0.091099	0.512127 (15)	-10.0	4.61	30.6	1.13	133 ± 31
< 0.1 micron																		
2134	7	0.1057	0.51230	-6.6	0.13068	0.512279 (9)	-7.0	11.6	53.8	15	14	0.10143	0.512302 (19)	-6.5	9.14	54.5	1.00	
2438	8	0.1072	0.51219	-8.7	0.13247	0.512198 (15)	-8.6	16.0	73.0	11	47	0.084848	0.512189 (13)	-8.8	1.37	9.79	1.01	
2743	9	0.1100	0.51223	-8.0	0.15125	0.512230 (10)	-8.0	15.8	63.0	8.8	41	0.081420	0.512234 (11)	-7.9	1.18	8.76	0.93	
3048	10	0.1083	0.51220	-8.5	0.18734	0.512282 (8)	-6.9	9.25	29.8	14	25	0.080402	0.512174 (9)	-9.1	1.95	14.6	0.99	
3048	10	0.1105	0.51220	-8.5	0.19079	0.512281 (12)	-7.0	11.4	36.1	15	33	0.080765	0.512170 (16)	-9.1	1.68	12.6	1.00	
3353	11	0.1052	0.51221	-8.3	0.18841	0.512245 (13)	-7.7	6.71	21.5	16	24	0.081398	0.512228 (9)	-8.0	1.72	12.8	0.94	
3658	12	0.0967	0.51224	-7.8	0.18580	0.512241 (6)	-7.7	8.02	26.1	11	20	0.082621	0.512235 (10)	-7.9	1.69	12.5	0.94	

a: untreated samples are calculated from weighted leachate and residue data.

b: sample numbers refer to well depth in thousands of feet.

c: calculated relative to $(^{143}Nd/^{144}Nd)_{CHUR} = 0.512638$.

d: wt.% leachate relative to untreated sample weight.

e: wt.% Nd leached relative to total Nd inventory.

f: Nd model age relative to depleted mantle source in Ga.

g: leachate-residue apparent ages, calculated using ISOPLOT [54].

are in present-day Nd isotopic equilibrium, and display $^{147}Sm/^{144}Nd$ ratios that differ by factors of 1.3 to 2.4 (Fig. 4b). The variation in present-day Nd isotopic compositions and $^{147}Sm/^{144}Nd$ of all samples as a function of stratigraphic depth is shown in Fig. 5a and b. Whole rock leachates show a range in $^{147}Sm/^{144}Nd$ from 0.1223 to 0.2158 as a smooth function of depth. The leachates of the < 0.1 μm fraction also display increasing $^{147}Sm/^{144}Nd$ with depth, ranging from 0.1309 to 0.1884. Sample residues define two distinct populations as well. Whole rock residues are characterized by $^{147}Sm/^{144}Nd$ ratios decreasing from 0.1077 to 0.0907 with depth, whereas the fine-grained clay residues have lower $^{147}Sm/^{144}Nd$ values between 0.1010 and 0.0804. These leachate and residue data were re-integrated by weight to estimate data for the unleached bulk samples: the resulting calculated whole rock $^{147}Sm/^{144}Nd$ ratios are between 0.113 and 0.116, whereas calculated $^{147}Sm/^{144}Nd$ ratios for the < 0.1 μm fraction are lower and range from 0.097 to 0.110 (Table 3).

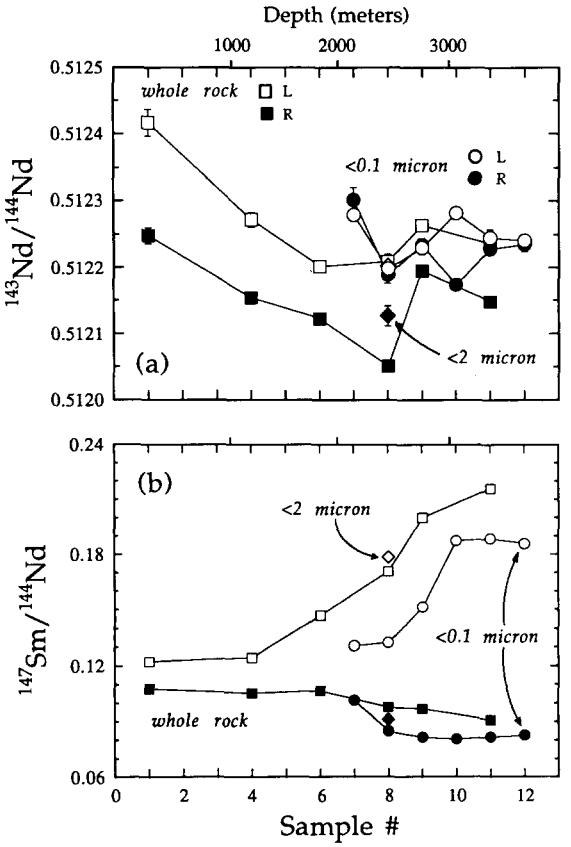

Fig. 5. (a) Variation of $^{143}Nd/^{144}Nd$ with depth. (b) Variation of $^{147}Sm/^{144}Nd$ with depth. Sample numbers denote well depth in thousands of feet. $^{143}Nd/^{144}Nd$ of whole rock residue–leachate pairs converge with depth, as their respective $^{147}Sm/^{144}Nd$ diverge. $^{143}Nd/^{144}Nd$ of < 0.1 μm leachate–residue pairs are identical (except sample 10), and their corresponding $^{147}Sm/^{144}Nd$ diverge as a function of depth.

7. Discussion

7.1. *Mineralogical constraints on the interpretation of the isotopic data*

The interpretation of the isotopic data is greatly facilitated by textural and chemical characterization of the separates. Size, texture and chemical composition of clay grains are parameters accessible by STEM. Below we briefly discuss the implications of these parameters as they pertain to the isotopic results and to the effects of acid leaching.

We consider the abundance of euhedral illite and the absence of detrital phases as strong evidence that the < 0.1 μm fraction approximates a mineral separate, rather than being just a size separate of questionable composition. In particular, no feldspar grains, fragments of feldspar, or anhedral smectite have been found, validating the completeness and the non-destructive character of the separation procedure employed. Hence observed isotopic variations can be directly related to processes involving authigenic clay. The absence of compositionally zoned clay and the occurrence of only one population of illite grains without distinct discontinuities in size and composition suggest that clay diagenesis involved a one-step process resulting in the formation of the presently observed phases. There is no evidence for protracted clay growth. Finally, euhedral or fragmented subhedral grain shapes suggest that illite precipitated from a fluid, and was not derived from solid state, layer-by-layer replacement of smectite within a pre-existing framework of detrital clay. This conclusion is consistent with the more extensive data set of Freed and Peacor [8].

The effect of acid leaching on the grains is difficult to evaluate from the STEM data alone. The dominant interlayer cation is K, yet the measured K is always insufficient to account for the calculated negative layer charge. Analytical data for alkalis are problematic and subject to error, as rapid diffusion of K parallel to the basal plane

(001) results in a net loss of alkali elements [38]. No general relationship between the calculated interlayer charge, the measured amount of K, and the size of the clay grains could be found. Only sample 8R displays a correlation between grain size and the actual amount of K lost (Table 1). Since the concentration of K is mainly affected by analytical diffusive loss, no useful information is available on its mobility during leaching. Comparison of the calculated interlayer charges before and after leaching is also inconclusive. Samples 8R and 8U display identical mean interlayer charges of 0.75 and 0.74 respectively, whereas the low mean of +0.65 for 11R (relative to +0.80 for 11U) would imply loss of Mg from the octahedral sites (assuming immobility of Al). Interestingly, sample 11R shows also a significantly higher deficiency of K relative to the calculated interlayer charge than the corresponding unleached sample 11U (Table 1). Both the apparent Mg and K mobility would imply that illite clay is not completely inert to leaching and, since cations in structural sites are not simply exchanging with H^+, in fact is partially dissolved by weak acids. In this case the Rb/Sr ratios of the clay will be maintained only if Rb and Sr are leached in proportional amounts, an assumption supported by the correlation of $^{87}Rb/^{86}Sr$ between leachates and untreated samples (Table 2).

7.2. *The origin of the leachable Sr*

The isotopic composition of the leachate is thought to be a function of the removal of Sr from soluble non-silicate phases such as calcite and apatite, and from clay-specific sites, namely exchangeable interlayer sites and basal surfaces. In addition, leaching of amorphous grain coatings of FeO(OH) may occur. X-ray diffraction analysis of unleached < 2 μm samples shows a gradual decrease of the calcite peak height from 1U to 5U, to being not detectable for the still deeper samples (R. Freed, pers. commun., 1990). The proportion of leached Sr is as high as 86% of the total Sr inventory for the shallowest samples, and decreases with depth, consistent with the disappearance of original calcite and the decrease in expandable layers of I/S clay (Fig. 1).

The $^{87}Sr/^{86}Sr$ ratio of 0.7076 for 1L is lower than the contemporaneous seawater isotopic composition of about 0.7085 [39]. As it is unusual to find post-depositional carbonate with $^{87}Sr/^{86}Sr$ that is lower than that of coeval seawater, we interpret the shallow leachate Sr isotopic compositions as resulting from a mixture of exchangeable Sr from detrital smectite (mostly volcanic-derived with low $^{87}Sr/^{86}Sr$ [40]), and Sr from dissolved skeletal carbonate. Leachates from shales shallower than 1830 m show approximately constant $^{87}Sr/^{86}Sr$ ratios, yet the age-equivalent seawater composition increases from 0.7076 to 0.7085 during Oligocene and Miocene time [39] (Fig. 1b). The anticipated decrease of $^{87}Sr/^{86}Sr$ with depth from dissolved calcite appears therefore to be balanced by increasing $^{87}Sr/^{86}Sr$ of Sr leached from the hydrated interlayers of the smectite-rich clay.

We interpret the Rb-Sr isochron as indicating that during illite growth all Sr in the clay–pore-fluid system largely equilibrated isotopically with $^{87}Sr/^{86}Sr$ of 0.7147. However, exchangeable Sr in leachates from greater than the clay transition depth has not maintained isotopic equilibrium with this system, preserved only in the non-exchangeable Sr component in the corresponding residues. Consequently a process is required that has lowered $^{87}Sr/^{86}Sr$ in leachable sites of the deeper samples to their present-day values of about 0.711, and that did not reset the non-exchangeable Sr in illite interlayers. It appears as if authigenic mixed-layer clays are partially open systems with respect to late resetting, and we suggest that their expandable interlayers act as pathways for continuing isotopic exchange, perhaps caused by the continuous interaction with less radiogenic waters fluxing the system (hence "exchangeable" Sr). In contrast, Sr that is firmly bound in non-expandable interlayers is not susceptible to late resetting, and has retained its initial Sr isotopic composition from the time of clay growth (hence "non-exchangeable" Sr). Evaluating the origin of leached Sr is clearly a complex subject. The correlation of $^{87}Sr/^{86}Sr$ of 8L through 12L (< 0.1 μm) with $^{87}Rb/^{86}Sr$ and $^{87}Sr/^{86}Sr$ of their corresponding residues (Table 2) may be indicative of a contribution of Sr from non-exchangeable sites as discussed in section 7.1 above. Finally, soluble diagenetic phases such as apatite in the deeper samples are a major source of leachable Sr as well. Leachable Sr certainly represents a mixture of Sr from all mentioned components; these compo-

nents are isotopically heterogeneous and the resulting mixing relationships reflect post-diagenetic resetting rather than an equilibrium composition.

The Sr isotopic depth profile resembles the mineralogical depth profile (Fig. 1) because exchangeable Sr in the shallow samples has never equilibrated in the authigenic system and instead has been dominated by less radiogenic Sr from carbonate and formation waters. In contrast, although exchangeable Sr in the deep samples has been lowered from the initial value of 0.7147 at 35 Ma to present intermediate values of about 0.709 to 0.711, elevated $^{87}Sr/^{86}Sr$ ratios of leachates from depths greater than the smectite/illite transition still bear evidence of radiogenic Sr in the authigenic system.

7.3. Rb-Sr isochrons and mixing lines

In a Rb-Sr isotopic evolution diagram such as Fig. 3, the sample complements U, R, and L must define a mass balance line. The slope of these lines can be considered Rb-Sr isochrons only if the isotopic composition of the leachate is close to that of the original system. In Fig. 3a the Rb-Sr isotopic data for the < 2 μm fraction are summarized, and we observe a non-systematic scatter of apparent residue–leachate ages between 105 and 249 Ma (Table 2), in excess of the depositional ages. This scatter can be explained either by the persistence of variable proportions of detrital grains introducing inherited Sr, or by isotopic disequilibrium between Sr in authigenic clay and the exchangeable Sr following illitization. The ages so obtained are geologically meaningless. Individual apparent residue–leachate ages from the < 0.1 μm fraction (Fig. 3b) range from 56 to 98 Ma (Table 2). There is no evidence for systematic change with depth as would be implied by protracted clay growth. Furthermore, we doubt the significance of these leachate–residue ages on several grounds:

(1) The ages either exceed or coincide with the depositional age, requiring at best syn-depositional illitization.

(2) Sr/Nd ratios in the leachates are between 20 and 100, greater than apatite Sr/Nd of typically less than 10, and hence imply a significant Sr contribution from exchangeable clay sites. These sites are prone to be isotopically reset in the presence of Sr-rich pore-fluids.

(3) If the residue isochron were merely a mixing line rather than due to in-situ decay since illitization, $^{87}Sr/^{86}Sr$ would have had to be negatively correlated with $^{87}Rb/^{86}Sr$. This is unlikely and no such correlation is apparent in the whole rocks residues at an apparent age of about 56 to 58 Ma (Table 2).

(4) Finally, as we believe the < 0.1 μm fraction to be devoid of contaminating detrital phases, we conclude that continued isotopic exchange has affected the exchangeable Sr reservoir. Two-point "isochrons" do not appear to give geologically meaningful illitization ages for the samples in question.

In contrast, we propose that the Rb-Sr isochron age of 34.8 ± 2.0 Ma for < 0.1 μm residues (Fig. 3b) dates an episode of illite crystallization over a considerable depth range. Only the illite-rich clays 8R through 12R from below the smectite/illite transition are included in the regression, whereas sample 7R is excluded as it is mineralogically different (Fig. 1a). The spread in $^{87}Rb/^{86}Sr$ ratios of the residues reflects sizable fractionation of the Rb-Sr system during diagenesis and we can envisage several processes that may control fractionation. Variable Rb/Sr ratios can be imparted from the whole rock system as detrital phases dissolve. Alternatively, the precipitation of Sr-rich accessory apatite can raise the Rb/Sr ratio in the residual fluid, a process consistent with the general increase of $^{87}Rb/^{86}Sr$ of $< 0.1\mu$m residues with depth and the concomitant increase of both $^{87}Sr/^{86}Sr$ and $^{147}Sm/^{144}Nd$ in the corresponding leachates (apatite having the initial Sr isotopic composition of 0.7147 and also high Sm/Nd ratios). Finally, the pore-fluid itself may fractionate during interaction with mixed-layer clay, as Sr is more easily hydrated and incorporated in expandable interlayers.

Support for the interpretation of episodic clay growth can be found in the study by Aronson and Hower [20] on rocks of the lower Frio Formation from a well in Harris County, Texas (Fig. 1). They obtained near constant K-Ar ages of about 33 to 35 Ma in the < 0.1 μm fraction of their deepest well samples. Consistent with a model of burial diagenesis involving solid-state transformation of smectite to illite, an age correction was applied to

allow for extant detrital smectite layers in the I/S clay, and the lack of increase in the K-Ar ages with depth was interpreted to reflect low-temperature diffusive loss of ^{40}Ar at higher temperature. In light of our data it is probable that these ages did not suffer from post-diagenetic resetting, but rather reflect an episodic event, although this would require growth of illite under near surface conditions. Morton [2] reached a similar conclusion using a Rb-Sr isochron of 23.6 Ma for illite from stratigraphically equivalent rocks. The results of both our study of Eocene to Paleocene shales and Morton's work on Oligocene shales [2] imply diagenesis at identical depths as shallow as 1200 m (Fig. 1b), consistent with low equilibrium temperatures (< 70°C) from O-isotope thermometry on I/S clay and quartz overgrowths [2,41]. Hence the difference in illitization age reflects the difference in depositional age and the subsequent burial history of the rocks.

The initial Sr isotopic composition of 0.7147 defined by the Rb-Sr isochron is more radiogenic than that of any of the leachates. The inferred composition of the pore-fluid is also higher than measured Sr isotopic ratios of Gulf Coast basin brines (e.g. [42–44]), which range from about 0.707 to 0.711. Such high $^{87}Sr/^{86}Sr$ of pore-fluids can be derived either from the introduction of more radiogenic basinal brines that have exchanged with sediment at depth, or from rock-dominated exchange in a near closed system (see section 7.5). The isotopic data presented here are compatible with either scenario, and both episodic influx of brines from the pre-Cenozoic basement [44] and the rock-domination of Gulf Coast basinal brines are widely discussed in the literature (e.g. [42–46]).

7.4. *Sm-Nd fractionation during diagenesis: potential for dating*

The studied diagenetic system is extremely young, and given the accuracy of the isotopic composition data and the observed difference in $^{147}Sm/^{144}Nd$ of a given residue–leachate pair, it is not possible to distinguish between Nd isotopic equilibrium at the present time and at a time < 40 Ma in the past. However, *if* isotopic equilibration occurred in that time span and *if* the system was subsequently not disturbed, apparent present-day equilibrium is expected.

The inverse correlation between leachate and residue $^{147}Sm/^{144}Nd$ is apparent in both whole rock and < 0.1 μm fractions (Fig. 5). Whole rock leachates from 305 m and 1220 m depth have $^{147}Sm/^{144}Nd$ ratios of 0.1223 and 0.1245, similar to modern seawater and carbonate [47]. The deeper whole rock leachates have higher $^{147}Sm/^{144}Nd$ up to 0.216, but not as high as values reported by Awwiller and Mack [48] (up to 0.346). The coupled Sm-Nd fractionation of residue–leachate pairs is clearly not a leaching effect, as we observe increased fractionation between both sample complements as a regular function of depth (Fig. 5b). This is probably caused by enhanced reaction rates and precipitation of a REE fractionating phase such as apatite at higher temperatures.

The progressive equilibration of leachates and residues is both a function of depth (Fig. 5), and decreasing grain size (Fig. 6). In both cases this is a result of the reconstitution of original detrital material to form new illite. Firstly, detrital minerals are dissolved with burial, and whole rock samples at depth are mainly (but not fully) comprised of authigenic minerals. Secondly, increasingly finer-grained size fractions are also enriched in authigenic minerals, and isotopic equilibrium between residues and leachates should be progressively attained. This is documented in the results for various grain sizes of sample 8 (Fig. 6). The leachates of the whole rock and of the < 2 μm

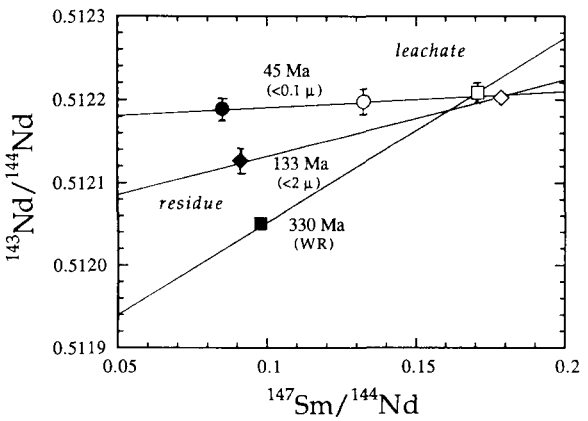

Fig. 6. Apparent ages of residue–leachate pairs for whole rock, < 2 mm and < 0.1 mm size fractions of sample 8 are younging with progressively smaller grain size. This results from the higher abundance of authigenic clay in the finer fractions. All leachates are in isotopic equilibrium with the < 0.1 μm fraction.

fraction plot on the extension of the "two-point isochron" defined by the < 0.1 μm residue–leachate pair, suggesting that leachable Nd in all size fractions was isotopically equilibrated with illite and, because of very low Nd concentrations in fluids, has not been reset since then. Consistent with the greater persistence of detrital phases with low $^{143}Nd/^{144}Nd$ in the coarser size fractions, the < 2 μm and the whole rock residues delineate progressively older apparent ages of 134 Ma and 330 Ma with their complementary leachates. The apparent < 0.1 μm Sm-Nd age of 45 ± 24 Ma is too imprecise to indicate anything other than young equilibration. However, this method may be useful for dating diagenesis and rock–fluid interaction in older rocks, as shown by preliminary results on Paleozoic sediments [49].

The underlying factors causing the observed Sm-Nd fractionation between leachates and residues are not entirely clear. Low $^{147}Sm/^{144}Nd$ ratios in the < 0.1 μm residues might indicate that authigenic illite incorporated Nd preferentially over Sm, leaving behind elevated Sm/Nd ratios in the fluid. This has also been suggested from whole rock Sm-Nd data on Wilcox shales [48]. Ionic radii for Sm^{3+} and Nd^{3+} in eight-fold coordination are 1.08 Aå and 1.10 Aå, respectively [50]. Given the similarity of ionic radii it is not very plausible to expect significant fractionation of Sm from Nd in interlayers of the phyllosilicate structure. Alternatively, Sm-Nd fractionation may be controlled by accessory phases that incorporate large amounts of REE in their structure. As small crystals of diagenetic apatite are commonly observed in the < 0.1 μm separates, and since middle REE substitute preferentially into its Ca sites [51,52], the high $^{147}Sm/^{144}Nd$ in the leachates could be caused by dissolution of even small amounts of apatite. Between 62% and 16% of the whole rock Nd inventory, and between 47% and 14% of the < 0.1 μm Nd inventory is leachable (Table 3). This suggests that an important proportion of the REE budget is sequestered in REE-rich accessory minerals such as apatite, and probably to a lesser degree either adsorbed onto grain surfaces or available in exchangeable interlayer sites.

We conclude that dissolution and precipitation processes during clay diagenesis involve isotopic homogenization of Nd on a sample scale, and that redistribution of the REE between cogenetic diagenetic phases such as illite and apatite causes pronounced Sm/Nd fractionation. This conclusion is at variance with the purported lack of mobility and geochemical fractionation of REE during diagenetic processes (e.g. [53]).

7.5. *Closed system versus open system diagenesis*

One can envisage two situations under which authigenic illite grows from a co-existing pore-fluid. One endmember scenario involves closed system conditions characterized by low fluid/rock ratios akin to previously suggested mechanisms of in-situ illitization (e.g. [1,18]). Alternatively, open system conditions could be established involving flow of fluids or diffusion of solutes through the rock as a means of introducing the reactants into the system. The two endmember situations can be tested using Sr and Nd isotopic data.

We use smectite-rich rocks above the smectite/illite transition as pre-diagenesis equivalents for rocks now below the transition. Such an approach is approximate at best as it implies that provenance and bulk chemical composition of the sediment are constant. An approximation for the ambient, pre-diagenetic Sr isotopic composition is $(^{87}Sr/^{86}Sr)_{35Ma}$ of whole rocks 4R and 6R. Their values of 0.717 and 0.719, respectively, are higher than the inferred initial $^{87}Sr/^{86}Sr$ of 0.7147, suggesting a contribution from less radiogenic brines to the authigenic system. It is easy to calculate a series of minimum bulk fluid/rock ratios using a simple mixing equation such as:

$$\left(\frac{\text{fluid}}{\text{rock}}\right)_{\text{bulk}} = \left[\frac{(R_m - R_r)}{(R_f - R_r)}\right] \cdot \left(\frac{C_r}{C_f}\right) \cdot \Delta D$$

where $R_m = {}^{87}Sr/{}^{86}Sr$ of the system following isotopic exchange between rock and fluid = 0.7147; $R_r = {}^{87}Sr/{}^{86}Sr$ of whole rocks 4R and 6R; $R_f = {}^{87}Sr/{}^{86}Sr$ of the original fluid; C_r = Sr concentration in rock; C_f = Sr concentration in fluid, ΔD = density factor = 2.4.

We assume a range of reasonable $^{87}Sr/^{86}Sr$ (0.7080 to 0.7105) and Sr concentrations (100 mg/l to 300 mg/l) for the pre-illitization pore-fluid [49–51], while keeping the Sr concentration in the rock fixed at 80 ppm (Table 2). High R_f (0.7105) and low C_f (100 mg/l) give rise to the highest

fluid/rock ratio at a given rock isotopic composition R_r. For $R_r = 0.717$, $(\text{fluid/rock})_{bulk}$ ranges from 0.22 to 1.05, and for $R_r = 0.719$, $(\text{fluid/rock})_{bulk}$ ranges from 0.41 to 1.97. The available pore space in argillaceous rocks is likely to be lower than the calculated minimum fluid/rock ratios, and we infer that open system conditions involved a moderate but not large flux of fluids into the rock column.

Fluids are extremely depleted in REE compared to silicate phases, and hence diagenetic systems with relatively low fluid/rock ratios are not expected to show any change in the Nd isotopic composition compared to the original rock. Values of $(^{143}Nd/^{144}Nd)_{35\ Ma}$ for the < 0.1 μm residues are between 0.51217 and 0.51222 (excluding sample 10), whereas shallow whole rock residues (4R and 6R) have marginally lower $(^{143}Nd/^{144}Nd)_{35\ Ma}$ of 0.51213 and 0.51210. A change in provenance with time could be responsible, but preferential dissolution of detrital smectite with relatively radiogenic Nd [48] and incorporation of this Nd component into precipitating illite may also explain the slightly higher $^{143}Nd/^{144}Nd$ in the < 0.1 μm residues. Another important consequence of the depletion of REE in pore-fluids is the preservation of Nd isotopic equilibrium on a sample scale. Continued interaction with such fluids will generally not change the isotopic composition in leachable sites, and, unlike for the Rb-Sr system, Sm-Nd leachate–residue dates can be expected to yield meaningful age information.

8. Concluding remarks

Rb-Sr data for leached authigenic illite indicate that illitization of smectite in Texas Gulf Coast shales occurred episodically tens of million years after deposition, and this event affected rocks over a considerable depth range. The diagenetic system was rock dominated, yet the heterogeneity in initial Sr isotopic compositions of diagenetic minerals was small relative to the variations imparted from in-situ decay of ^{87}Rb. This allows dating of diagenesis on a local scale. The observed present-day Nd isotopic equilibrium and significant Sm-Nd fractionation in the fine fractions is attributed to redistribution of REE during clay diagenesis, possibly controlled by cogenetic accessory phases rich in REE, such as apatite. Since pore-fluids are depleted in REE, the Sm-Nd system will generally be robust with respect to late resetting and we therefore suggest the possibility of single-sample Sm-Nd dating of very low-grade sediments of sufficient age (> 400 Ma). Such a single-sample approach is superior to multi-sample isochrons because the effect of initial isotopic heterogeneity is eliminated. Finally, the inferred timing of episodic diagenesis at 35 Ma requires illitization to have taken place at shallow depths between 1200 m and 2400 m, and temperatures not exceeding approximately 70°C.

Acknowledgments

This research was supported by NSF grants EAR-8804072 to A.N.H., EAR-8817080 to D.R.P., and EAR-9005516 to D.R.P. and A.N.H.. M.O. acknowledges the receipt of a Ph.D. fellowship from the Studienstiftung des Deutschen Volkes. Drill cuttings and < 2 μm size fractions were kindly provided by R.L. Freed. R. Keller is thanked for technical assistance. L.M. Walter, E.J. Essene and B.H. Wilkinson commented on an earlier version of the manuscript. We also thank C. Smalley, C. Hawkesworth, and an anonymous referee for helpful comments, and L. Land for discussion.

References

1 J. Hower, E.V. Eslinger, M.H. Hower and E.A. Perry, Mechanism of burial metamorphism of argillaceous sediments, 1. Mineralogical and chemical evidence, Geol. Soc. Am. Bull. 87, 725–737, 1976.
2 J.P. Morton, Rb-Sr evidence for punctuated illite/smectite diagenesis in the Oligocene Frio Formation, Texas Gulf Coast, Geol. Soc. Am. Bull. 96, 114–122, 1985.
3 J. Oliver, Fluids expelled tectonically from orogenic belts: their role in hydrocarbon migration and other geological phenomena, Geology 14, 99–102, 1986.
4 J.H. Ahn and D.R. Peacor, Transmission and analytical electron microscopy of the smectite to illite transition, Clays Clay Miner. 34, 165–179, 1986.
5 J.F. Burst, Diagenesis of Gulf Coast clayey sediments and its possible relation to petroleum migration, Bull. Am. Assoc. Pet. Geol. 53, 73–93, 1969.
6 E.A. Perry and J. Hower, Burial diagenesis in Gulf Coast pelitic sediments, Clays Clay Miner. 18, 165–177, 1970.
7 R.L. Freed, Clay mineralogy and depositional history of the Frio Formation in two geopressured wells, Brazoria county, Texas, Gulf Coast Assoc. Geol. Soc. Trans. 32, 459–463, 1982.

8 R.L. Freed and D.R. Peacor, Diagenesis and the formation of illite-rich I/S crystals in Gulf Coast shales: TEM study of clay separates, J. Sediment. Petrol., in press, 1991.
9 J.R. Boles and S.G. Franks, Clay diagenesis in the Wilcox sandstone of southwest Texas: implications of smectite diagenesis on sandstone cementation, J. Sediment. Petrol. 49, 55–70, 1979.
10 J.H. Lee, D.R. Peacor, D.D. Lewis and R.P. Wintsch, Evidence for syntectonic crystallization for mudstone to slate transition at Lehigh Gap, Pennsylvania, U.S.A., J. Struct. Geol. 8, 767–780, 1986.
11 W.T. Jiang, E.J. Essene and D.R. Peacor, Transmission electron microscopic study of coexisting pyrophyllite and muscovite: direct evidence for the metastability of illite, Clays Clay Miner. 38, 225–240, 1990.
12 A. Baronnet, Ostwald ripening in solution. The case of calcite and mica, Estud. Geol. 38, 185–198, 1982.
13 D.D. Eberl, J. Srodon, M. Kralik, B.E. Taylor and Z.E. Peterman, Ostwald ripening of clays and metamorphic minerals, Science 248, 474–477.
14 S.D. McDowell and W.A. Elders, Authigenic layer silicate minerals in borehole Elmore 1, Salton Sea Geothermal Field, California, U.S.A., Contrib. Mineral. Petrol. 74, 293–310, 1980.
15 E.V. Eslinger and B. Sellars, Evidence for the formation of illite from smectite during burial metamorphism in the Belt Supergroup, Clark Fork, Idaho, J. Sediment. Petrol. 51, 203–216, 1981.
16 H. Dypvik, Clay mineral transformations in Tertiary and Mesozoic sediments from the North Sea, Bull. Am. Assoc. Pet. Geol. 67, 160–165, 1983.
17 A.A. Aldahan and S. Morad, Mineralogy and chemistry of diagenetic clay minerals in Proterozoic sandstones from Sweden, Am. J. Sci. 286, 29–80, 1986.
18 H. Kisch, Mineralogy and petrology of burial diagenesis (burial metamorphism) and incipient metamorphism of clastic rocks, in: Diagenesis in Sediments and Sedimentary Rocks, 2. Developments in Sedimentology 25B, G. Larsen and G.V. Chilingar, eds., pp. 289–494, Elsevier, Amsterdam, 1983.
19 J.P. Morton, Rb-Sr dating of diagenesis and source age of clays in Upper Devonian black shales of Texas, Geol. Soc. Am. Bull. 96, 1043–1049, 1985.
20 J.L. Aronson and J. Hower, Mechanism of burial metamorphism of argillaceous sediment, 2. Radiogenic argon evidence, Geol. Soc. Am. Bull. 87, 738–744, 1976.
21 J.C. Hunziker, M. Frey, N. Clauer, R.D. Dallmeyer, H.D. Friedrichsen, W. Flehming, K. Hochstrasser, P. Roggweiler and H. Schwandner, The evolution of illite to muscovite: mineralogical and isotopic data from the Glarus Alps, Switzerland, Contrib. Mineral. Petrol. 92, 157–180, 1986.
22 W.C. Elliott and J.L. Aronson, Alleghenian episode of K-bentonite illitization in the southern Appalachian basin, Geology 8, 735–739, 1987.
23 N. Liewig, N. Clauer and F. Sommer, Rb-Sr and K-Ar dating of clay diagenesis in Jurassic sandstone oil reservoir, North Sea, Am. Assoc. Pet. Geol. Bull. 71, 1467–1474, 1987.
24 M. Lee, J.L. Aronson and S.S. Savin, Timing and conditions of Permian Rotliegende sandstone diagenesis, southern North Sea: K/Ar and oxygen isotopic data, Am. Assoc. Pet. Geol. Bull. 73, 195–215, 1989.
25 M.E. Erwin and L.E. Long, Rb-Sr ages of diagenesis of Mg-rich clay, Permian evaporite sequence, Palo Duro Basin, Geol. Soc. Am. Prog. Abstr. 21, A-17, 1989.
26 N. Clauer, J.R. O'Neil, C. Bonnot-Courtois and T. Holtzapffel, Morphological, chemical, and isotopic evidence for an early diagenetic evolution of detrital smectite in marine sediments, Clays Clay Miner. 38, 33–46, 1990.
27 P.R. Whitney and P.M. Hurley, The problem of inherited radiogenic strontium in sedimentary age determinations, Geochim. Cosmochim. Acta 28, 425–436, 1964.
28 A.W. Hofmann, J.W. Mahoney and B.J. Giletti, K-Ar and Rb-Sr data on detrital and postdepositional history of Pennsylvanian clay from Ohio and Pennsylvania, Geol. Soc. Am. Bull. 85, 639–644, 1974.
29 J.L. Aronson and M. Lee, K/Ar systematics of bentonite and shale in contact metamorphic zone, Cerrillos, New Mexico, Clays Clay Miner. 34, 483–487, 1986.
30 A.N. Halliday and J.G. Mitchell, K-Ar ages of clay concentrates from Irish orebodies and their bearing on the timing of mineralisation, Trans. R. Soc. Edinburgh 74, 1–14, 1983.
31 N. Clauer, A new approach to Rb-Sr dating of sedimentary rocks, in: Lectures in Isotope Geology, E. Jaeger and J.C. Hunziker, eds., pp. 30–51, Springer-Verlag, Berlin, 1979.
32 N. Clauer, The Rb-Sr method applied to sediments: certitudes and uncertainties, in: Numerical Dating Methods in Stratigraphy, 2 Vols., G.S. Odin, ed., pp. 245–276. John Wiley, Chichester, 1982.
33 R.L. Freed and D.R. Peacor, TEM lattice fringe images with R1 ordering of illite/smectite in Gulf Coast pelitic rocks, Geol. Soc. Am. Prog. Abstr. 21, A16, 1989.
34 A.N. Halliday, G.A. Mahhod, P. Holden, J.M. Metz, T.J. Dempster and J.P. Davidson, Evidence for long residence times of rhyolitic magma in the Long Valley magmatic system: the isotopic record in precaldera lavas of Glass Mountain, Earth Planet. Sci. Lett. 94, 274–290, 1989.
35 M.L. Jackson, Soil Chemical Analysis—Advanced Course, 895 pp., Univ. Wisconsin Press, Madison, Wisc., 1969.
36 M. Kralik, Effects of cation-exchange treatment and acid leaching on the Rb-Sr system of illite from Fithian, Illinois, Geochim. Cosmochim. Acta 48, 527–533, 1984.
37 S. Chauduri and D.G. Brookins, The Rb-Sr systematics in acid leached clay minerals, Chem. Geol. 24, 231–242, 1979.
38 B.A. van der Pluijm, J.H. Lee and D.R. Peacor, Analytical electron microscopy and the problem of potassium diffusion, Clays Clay Miner. 36, 498–504, 1988.
39 D.J. DePaolo, Detailed record of Neogene Sr isotopic evolution of seawater from DSDP site 590B, Geology 14, 103–106, 1986.
40 C.D. Winkler, Cenozoic shelf margins, northwestern Gulf of Mexico, Gulf Coast Assoc. Geol. Soc. Trans. 32, 427–444, 1982.
41 H-W Yeh and S.M. Savin, Mechanism of burial metamorphism of argillaceous sediments, 3. O-isotope evidence, Geol. Soc. Am. Bull. 88, 1321–1330, 1977.
42 H.H. Posey, A.L. Workman, J.S. Hanor and S.D. Hurst,

Isotopic characteristics from three oil and gas fields, southern Louisiana, Gulf Coast Assoc. Geol. Soc. Trans. 35, 261–267, 1985.
43 A.M. Stueber, P. Pushkar and E.A. Hetherington, A strontium isotopic study of Smackover brines and associated solids, southern Arkansas, Geochim. Cosmochim. Acta 48, 1637–1649, 1984.
44 R.A. Morton and L.S. Land, Regional Variation in formation water chemistry, Frio Formation (Oligocene), Texas Gulf Coast, Am. Assoc. Pet. Geol. Bull. 71, 191–206, 1987.
45 R.S. Fisher and L.S. Land, Diagenetic history of Eocene Wilcox Sandstone, south-central Texas, Geochim. Cosmochim. Acta 50, 551–561, 1986.
46 R.K. Stoessel and C.H. Moore, Chemical constraints and origin of four groups of Gulf Coast reservoir fluids, Am. Assoc. Pet. Bull. 67, 896–906, 1983.
47 H. Elderfield and M.J. Greaves, The rare earth elements in sea water, Nature 296, 214–219, 1982.
48 D.N. Awwiller and L.E. Mack, Diagenetic resetting of Sm-Nd isotope systematics in Wilcox Group sandstones and shales, San Marcos Arch, south-central Texas, Gulf Coast Assoc. Geol. Soc. Trans. 39, 321–330, 1989.
49 M. Ohr, A.N. Halliday and D.R. Peacor, Sm-Nd studies of very low-grade sediments: timing of deposition and metamorphism, Abstr., Prog. Europ. Union Geosci., 1991.
50 D.G. Brookins, Aqueous geochemistry of rare earth elements, in: Geochemistry and Mineralogy of Rare Earth Elements: Reviews in Mineralogy, 21, B.R. Lipin and G.A. McKay, eds., pp. 201–223, 1989.
51 J.L. Drinkwater, G.K. Czamanske and A.B. Ford, Apatite of the Dufek Intrusion: distribution, paragenesis and chemistry, Can. Mineral. 28, 835–854, 1990.
52 P. Grandjean and F. Albarede, Ion probe measurement of rare earth elements in biogenic phosphates, Geochim. Cosmochim. Acta 53, 3179–3183, 1990.
53 S. Chauduri and R.L. Cullers, The distribution of rare-earth elements in deeply buried Gulf Coast sediments, Chem. Geol. 24, 327–338, 1979.
54 K.R. Ludwig, U.S. Geol. Surv. Open-File Rep. 88–557 (revision 3 January 1990), 1990.